Military Technical College
Kobry El-Kobbah,
Cairo, Egypt.

13th International Conference on Applied Mechanics and Mechanical Engineering.

IMPLEMENTATION OF ELECTRO-HYDRAULIC SERVO-VALVE FOR MODULATION OF THE ROCKET THRUST

RATEB* R.A., RABIE** M.G. and ELSENBAWI* M.A.

ABSTRACT

The modulation of the rocket thrust is required for many practical applications regarding certain missions to be performed by the missile. An existing thrust controller with two modes of operation has been studied and analyzed. To upgrade the controller to acquire a continuous gradual thrust modulation, an Electro-Hydraulic Servo-Pressure Controller (EHSPC) has been integrated with the system after making necessary adaptation of the current design. The valve parameters: controlled pressure, input pressure, pilot pressure variations, and input controlling current have been investigated and compared for the two systems using MATLAB SIMULINK program. It was possible to acquire a new system capable of performing a continuous thrust modulation while keeping the other characteristics of the system before modification.

KEY WORDS

Liquid Propellant Rocket Engine, Thrust Controller, Electro-Hydraulic Servo-valve, and Thrust Modulation.

NOMENCLATURE

A_{AS}	Openning area of port AS, m^2.	A_{BS}	Openning area of port BS, m^2.
A_{cp2}	Clear pisron area, m^2.	A_{CS}	Openning area of port CS, m^2.
A_{DS}	Openning area of port DS, m^2.	A_{e2}	Poppet area subjected to P_{otce}, m^2.
A_{i2}	Poppet area subjected to P_{op}, Pa.	A_N	Large poppet area, m^2.
A_{oS}	Fixed orifice area, m^2.	A_P	Small poppet area, m^2.
A_{pis}	Back piston area. m^2.	A_{SS}	Spool cross-sectional area, m^2.
A_{thr}	Throat area, m^2.	A_{5S}	Drain orifice area, m^2.
B_{oil}	Bulk modules of he oil, Pa.	C^*	Characteristics velocity.
C_C	Contraction coefficient	C_d	Discharge coefficient.
C_F	Thrust Coefficient.	d_{fS}	Flapper nozzle diameter; mm
d_N	Poppet large diameter, m.	d_p	Poppet small diameter, m.
d_S	Valve throttling diameter, m.	d_{SS}	Spool diameter, m.

---

* Egyptian Armed Forces.
** Professor, Modern Academy of Engineering and Technology.

d_V	Mean seat diameter, m.	F	Thrust, N.
F_{jS}	Hydraulic momentum force, N.	F_{L2}	Moving part displacement limmiter.
F_{SS}	Force acting at the extremity of the feed back spring, N.	f_{SS}	Spool friction coefficient, Ns/m.
f_2	Moving part friction coefficient Ns/m.	$f_{\theta S}$	Damping coefficient, Nms/rad.
I_{sp}	Specific impulse.	i_S	Torque motor input control carrunt.
J_S	Moment of inertia of the rotating parts; armature and flapper, Nms^2	K_{LfS}	Equivalent flapper seat stiffness, Nm.
K_{SS}	Stiffness of the feed back torque, N/m.	K_{S2}	Main spring stiffness, N/m.
K_{TS}	Stiffness of the Flexible tube, Nm/rad.	L_{fS}	Flapper length, mm
L_{SS}	Length of the feed back spring and flapper, mm.	L_s	Armature length; m.
$\dot{m}_{exit}$	Exit flow rate, Kg/s.	M_2	Moving parts mass for the modified thrust controller, Kg.
m_2	Moving parts mass for the current thrust controller, Kg.	P_C	Combustion chmber pressure, bar.
P_{og}	Oxidizer pressure at inlet of gas generator, Pa.	P_{op}	Valve inlet pressure, Pa.
P_{otce}	Valve outlet pressure, Pa.	P_{SS}	Supply pressure, Pa.
P_{TS}	Valve return pressure, Pa.	P_{1S}	Pressure in the left side of the flapper valve, Pa.
P_{2S}	Pressure in the right side of the flapper valve, Pa.	P_{3S}	Pressure in the flapper valve return chamber, Pa.
Q_{AS}	Volumetric flow rate at port AS, m^3/s.	Q_{BS}	Volumetric flow rate at port BS , m^3/s.
Q_{CS}	Volumetric flow rate at port CS, m^3/s.	Q_{DS}	Volumetric flow rate at port DS, m^3/s.
Q_{og}	Oxidizer flow rate at the inlet of gas generator, m^3/s.	Q_{otce}	Valve outlet flow rate, m^3/s.
Q_{otci}	Valve inlet flow rate, m^3/s.	Q_{1S}	Flow rate in the left orifice, m^3/s.
Q_{2S}	Flow rate in the right orifice, m^3/s.	Q_{3S}	Left flapper nozzle flow rate, m^3/s.
Q_{5S}	Flapper valve drain flow rate, m^3/s.	R_{fS}	Equivalent flapper seat damping coefficient, Nms/rad.
T_{FS}	Feed back torque, Nm	T_{L1S}	Torque due to flapper displacement limiter, Nm.
T_{PS}	Torque due to pressure forces, Nm.	T_S	Output mechanical torque of the EMTM.
V_{e2}	Exit chamber volume, m^3.	V_{oS}	Initial volume of the oil in the hydraulic amplifier line side, m^3.
V_{3S}	Volume of the flapper valve return line, m^3.	W_{eff}	Effective exhaust velocity, m/s.
X_{fLS}	Maximum flapper displacement, m.	X_{fS}	Flapper displacement, m.
X_{fs}	Flapper displacement on the level of the jet nozzles, m	X_{iS}	Initial flapper nozzle opening, m.
X_{m2}	Limiting displacement, m.	X_{SS}	Spool displacement, m.
X_{02}	Main spring pre-compression distance.	Δ_S	Spool radial clearance, m.
ω_S	Width of port on the valve sleeve, m.	θ_s	Armature rotation angle, rad
ρ_{oil}	Oil density, Kg/m^3.	ρ_{oS}	Oil density, Kg/m^3.

INTRODUCTION

For a liquid propellant rocket engine (LPRE), it is possible to obtain changes in the thrust magnitude. Thrust magnitude changes are also known as thrust modulation. Thrust modulation control is required in different ranges:

Up to 1:2 for avoiding too high acceleration during lunching phase
Up to 1:10 for lunar or planetary landing
Up to 1:100 when operating at low thrust for rendezvous

The thrust of (LPRE) can be expressed in the following form.

$$F = \dot{m}_{exit} \cdot W_{eff} = \frac{P_C A_{thr}}{C^*} \cdot I_{sp} = C_F \cdot P_C \cdot A_{thr} \qquad \textbf{(1)}$$

There are a number of alternative methods for controlling the magnitude of the thrust i is possible to change Specific impulse, Combustion pressure, Throat area, and Exit flow rate while Characteristics velocity is nearly constant (depending on the phenomena of combustion). In the present study the control thrust magnitude is achieved by controlling the combustion pressure [1, 2].

The various elements of the system will be described and detailed analysis of the modification to get a continues thrust modulation.

THRUST CONTROLLER

The thrust controller maintains the required pressure in the combustion chamber during the engine operation, and changes the engine over from the first power rating to the second one. The thrust controller controls the pressure of the oxidizer at the inlet of the gas generator to maintain the pressure in the combustion chamber. Figure (1-b) represents a function symbol of the thrust controller.

Pressure signal from the combustion chamber is fed to connector (**S**) of body (**5**), Fig (1-a), and acts on piston (**6**). When controllable pressure (pressure in the combustion chamber) is increased, piston (**6**), poppet (**4**), and valve (**2**), move toward spring (**8**) reducing the throttling passage and consequent drop in turbine and pump speed. The combustion chamber pressure drops to a preset value. When the controllable pressure reduces all processes proceed in reverse order. The operating pressures of the thrust controller are given in Table (1).

Mathematical Model

The mathematical model describing the controller dynamic behavior is deduced based on the scheme of Fig (1-a) under the following assumptions [3].

1- The effect of the transmission lines is neglected.
2- The pressure losses in these lines are negligible compared with the losses in the valve throttling elements. Their transient response is much faster than the valve moving parts.
3- Internal leakage through radial clearances between the piston (**6**) and the body (**9**) is neglected.

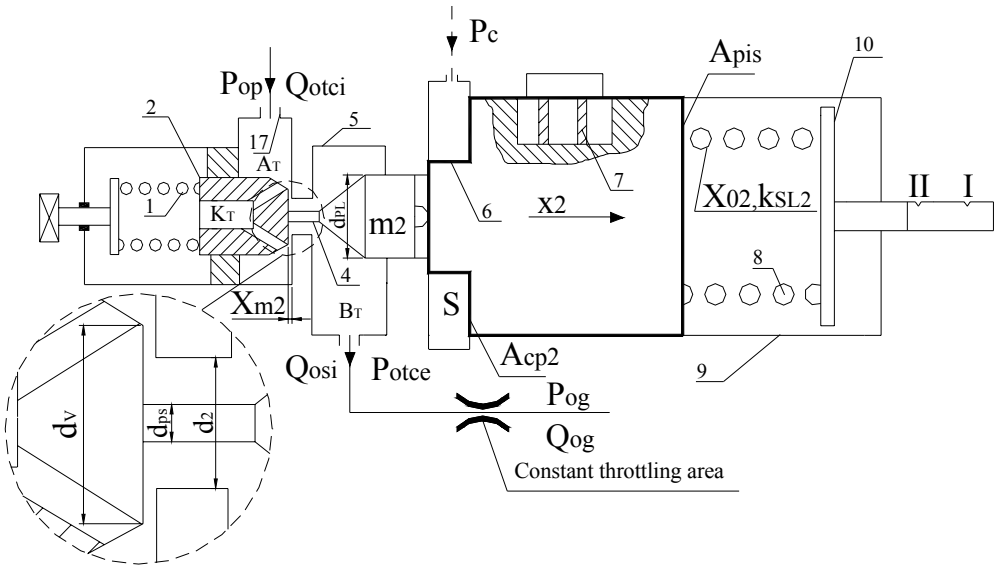

a- Scheme

1-Auxiliary spring; 2-Valve; 4-Poppet; 5-Controller body; 6-Piston; 7-Half-rings; 8-Adjusting spring; 9-Casing; 10-Disc; 17-Connector for oxidizer inlet from pump; π-Connector for combustion chamber pressure signal.

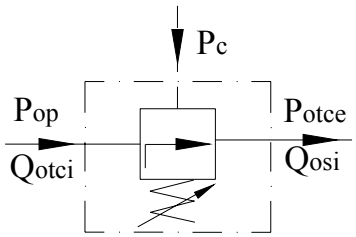

b- Symbol

Fig. (1) Thrust controller: a- Scheme, b- Symbol

Table (1) Numerical values of feeding pressure

Parameter	Firs rating	Second rating
Pressure in the combustion chamber (bar).	50	24.6
Oxidizer pressure at thrust controller inlet (bar).	81	31.8
Oxidizer pressure at controller outlet (bar).	63.5	18

Flow Rate Through Valve Orifice

The flow rate is expressed by:

$$Q_{otci} = C_d \pi d_V (X_{m2} - x_2)\sqrt{\frac{2}{\rho_o}(P_{op} - P_{otce})} \qquad \textbf{(2)}$$

where $\pi d_V(X_{m2}-x_2)$ is the smallest restriction area. the displacement (x_2) moves within the limits ($0<x_2<X_{m2}$).

Exit flow rate

The oxidizer flows from the thrust controller to the gas generator through a fixed throttling area as shone in Fig (1-a). Outlet flow rate can be expressed as follow.

$$Q_{osi} = K_d \sqrt{P_{otce} - P_{og}} \quad \textbf{(3)}$$

Applying continuity to exit chamber

The balance of flow rate in the valve cavity is expressed by.

$$Q_{otci} - Q_{osi} - A_N \frac{dx_2}{dt} = \frac{d}{dt}\left[\frac{V_{e2} + x_2 A_N}{B} P_{otce}\right] \quad \textbf{(4)}$$

Equation of motion of the moving parts

The following equation expressed the moving part equation of motion under pressure, and spring actions

$$P_C A_{cp2} + P_{otce} A_{e2} + P_{op} A_{i2} = m_2 \frac{d^2 x_2}{dt^2} f_2 \frac{dx_2}{dt} + K_{SL2}(x_2 + X_{02}) - F_{L2} \quad \textbf{(5)}$$

$$F_{LL2} = \begin{cases} |x_2| K_{L2} - f_{L2} \dfrac{dx_2}{dt} & x_2 \le 0 \\ 0 & x_2 > 0 \end{cases} \quad \textbf{(6.a)}$$

$$F_{LR2} = \begin{cases} (x_2 - X_{m2}) K_{L2} + f_{L2} \dfrac{dx_2}{dt} & x_2 \ge X_{m2} \\ 0 & x_2 < X_{m2} \end{cases} \quad \textbf{(6.b)}$$

$$F_{L2} = F_{LL2} - F_{LR2} \quad \textbf{(6)}$$

MODIFIED THRUST CONTROLLER

The purpose of the modification is to get a continuous thrust modulation. The modified thrust controller, Fig (2), is designed to operate at the same operating conditions and to perform the same function of the current thrust controller. The heavy spring (**8**) is removed, and its function is secured by a pressurized chamber. The control in the pressure in this chamber will result in flow regulation.

Mathematical Model

The equations **(2)**, **(3)**, **(4)**, and **(6)** are valid for the modified thrust controller. The equation of motion of the moving parts **(5)** will be expressed as.

$$P_C A_{cp2} + P_{otce} A_{e2} + P_{op} A_{i2} = m_2 \frac{d^2 x_2}{dt^2} f_2 \frac{dx_2}{dt} + P_{ctl} A_{pis} - F_{L2} \quad \textbf{(7)}$$

Simulation

Figures (3) to (9), shows a simulation sample of thrust controller before and after simulation. These figures show the controller exit oxidizer pressure ($\mathbf{P_{otce}}$) variation with

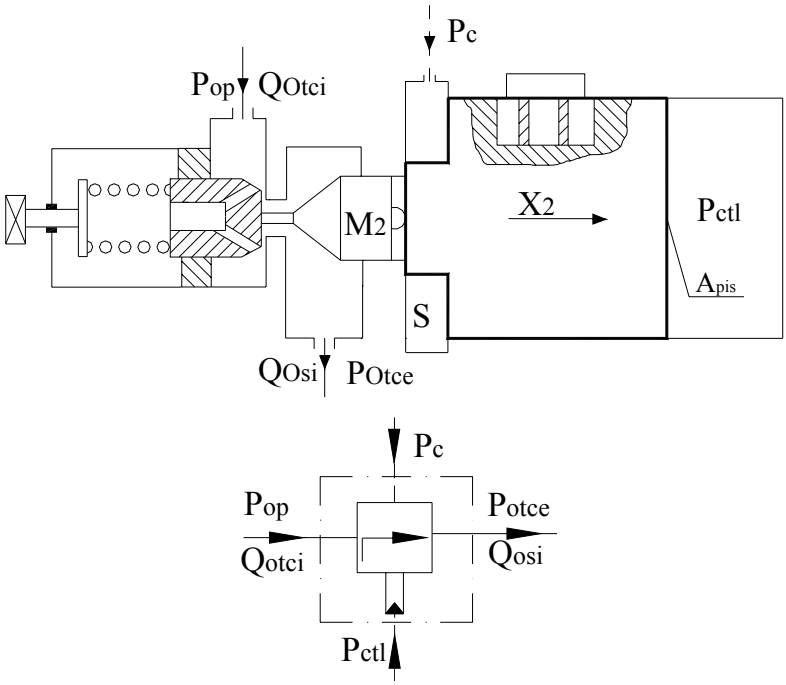

a- scheme

b- symbol

Fig. (2) Modified thrust controller: a- Scheme, b-Symbol

step variations of pre-compression length ($\mathbf{X_{02}}$) of the heavy spring (**8**), controlable pressure ($\mathbf{P_{ctl}}$), input oxidizer pressure ($\mathbf{P_{op}}$), and combustion chamber pressure signal ($\mathbf{P_C}$). This figure shows also a comparison between each controller's responses due to different input signals.

The pre-compression length ($\mathbf{X_{02}}$) of the spring (**8**), Fig (1-a), is the only adjustable constructional parameters in the thrust controller. The exit oxidizer pressure ($\mathbf{P_{op}}$) response before modification due to spring precompression length ($\mathbf{X_{02}}$) step variations was plotted in Fig (3). Figure (4) represents the exit oxidizer pressure ($\mathbf{P_{op}}$) response after modification due to controlling pressure ($\mathbf{P_{ctl}}$) step variations. The comparison between thrust controller exit oxidizer pressure ($\mathbf{P_{op}}$) responses before and after modification is plotted in Fig (5). By study Fig (3), Fig (4), and Fig (5) the current thrust controller and the modified thrust controller responses are the same from point of view steady sate error, and overdamped response, but with a little change in the settling time.

The effect of input oxidizer pressure ($\mathbf{P_{op}}$) was studied for thrust controllers. Figure (6) & Fig (7) represent each controller response due to ($\mathbf{P_{op}}$) step variation, and Fig (8) represents a comparison between each controller due to ($\mathbf{P_{op}}$) step variation. The study of, Fig (8) & Fig (9) shows that the exit oxidizer pressure ($\mathbf{P_{otce}}$) in both controllers retain the nominal value after any change of inlet oxidizer pressure ($\mathbf{P_{op}}$), means that both thrust controllers would maintain the exit oxidizer pressure ($\mathbf{P_{otce}}$) for any flight trajectory rating.

The comparison between both controllers due to input oxidizer pressure ($\mathbf{P_{op}}$) step variations is plotted in Fig (8). By studying this figure the modified thrust controller has the same response behavior, but with slightly changes in the steady state error as compared to the current controller.

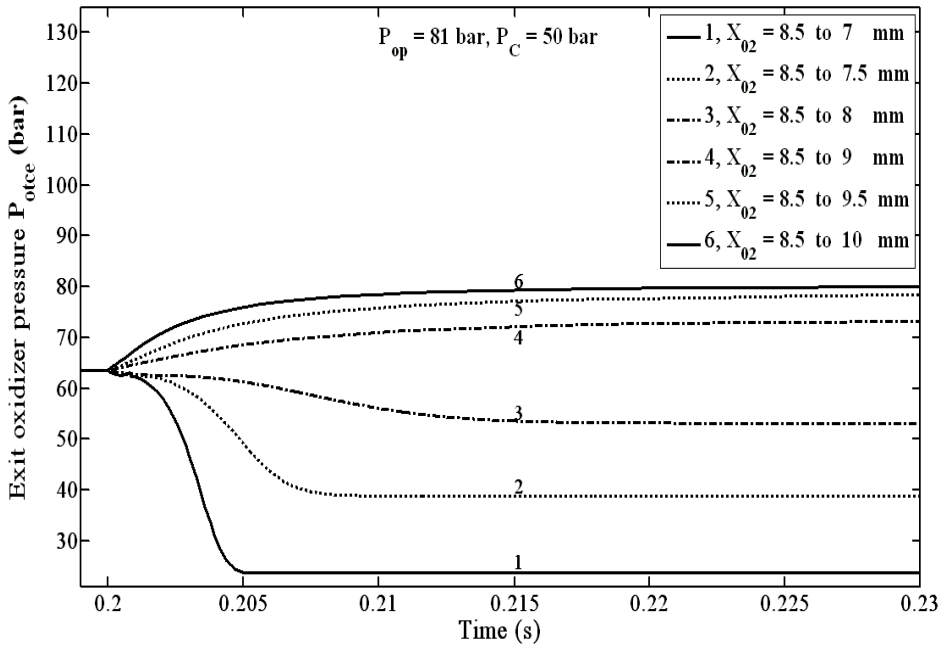

Fig. (3) Response of the thrust controller exit pressure (P_{otce}) to spring precompression length X_{02} step variation.

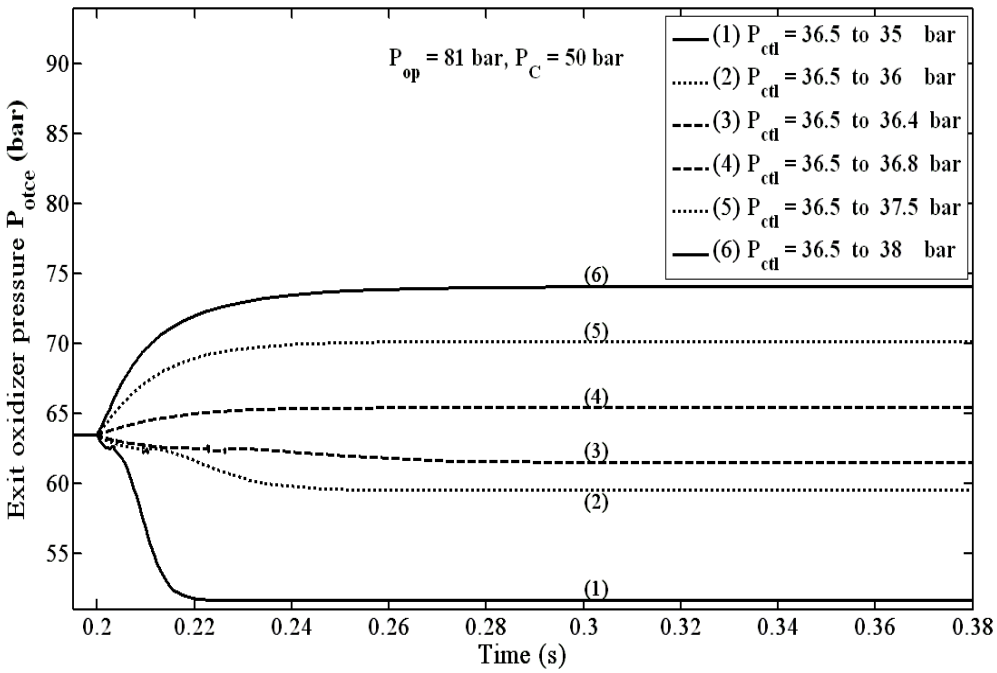

Fig. (4) Response of the modified thrust controller exit pressure (P_{otce}) to controlling pressure (P_{ctl}) step variation.

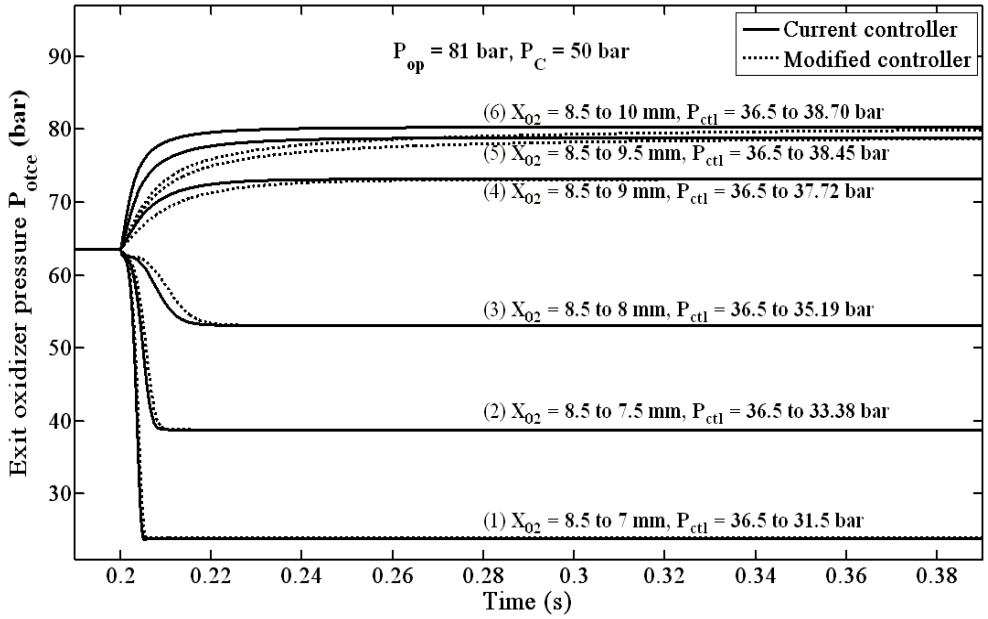

Fig. (5) Comparison between the modified, and the current thrust controller responses due to (X_{02}), and (P_{ctl}) step variation.

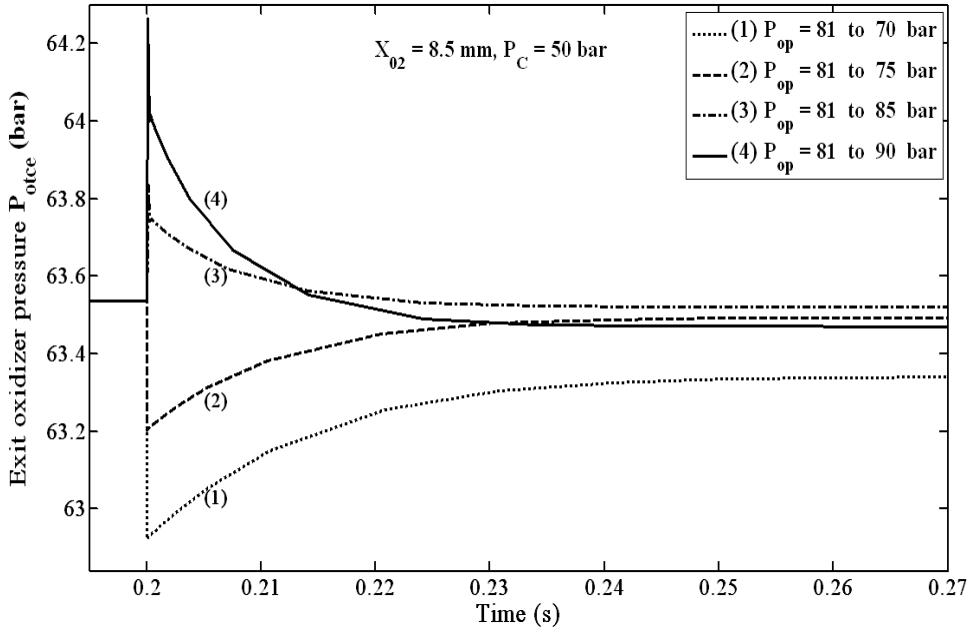

Fig. (6) Response of the thrust controller to input oxidizer pump pressure (P_{op}) step variation.

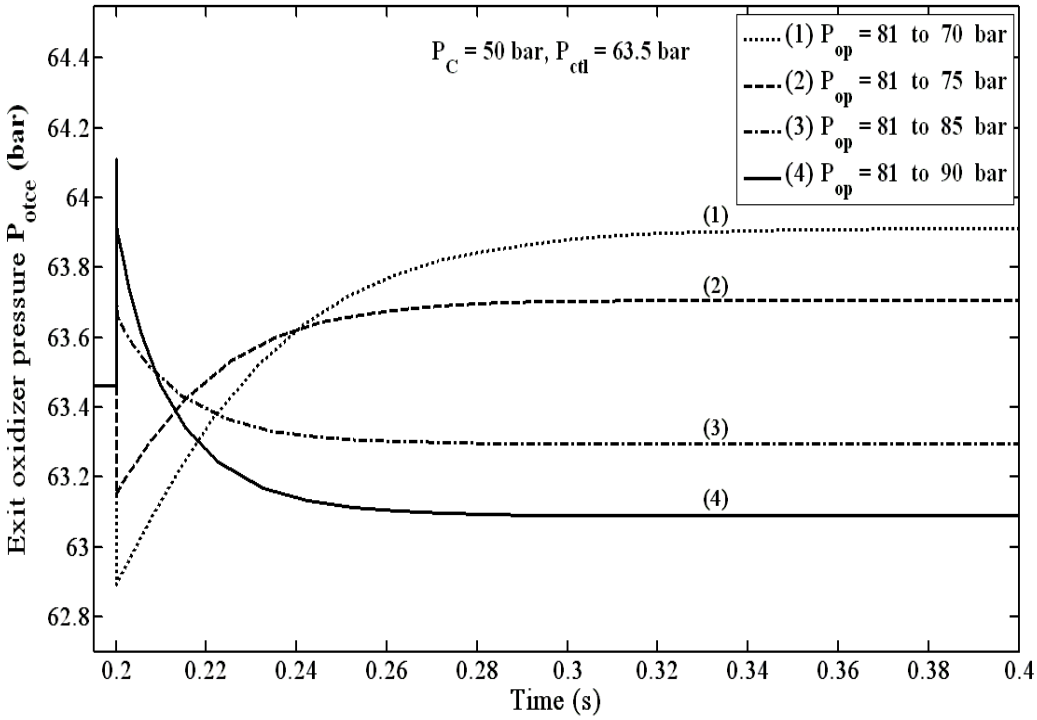

Fig. (7) Response of the modified thrust controller to input oxidizer pump pressure (P_{op}) step variation.

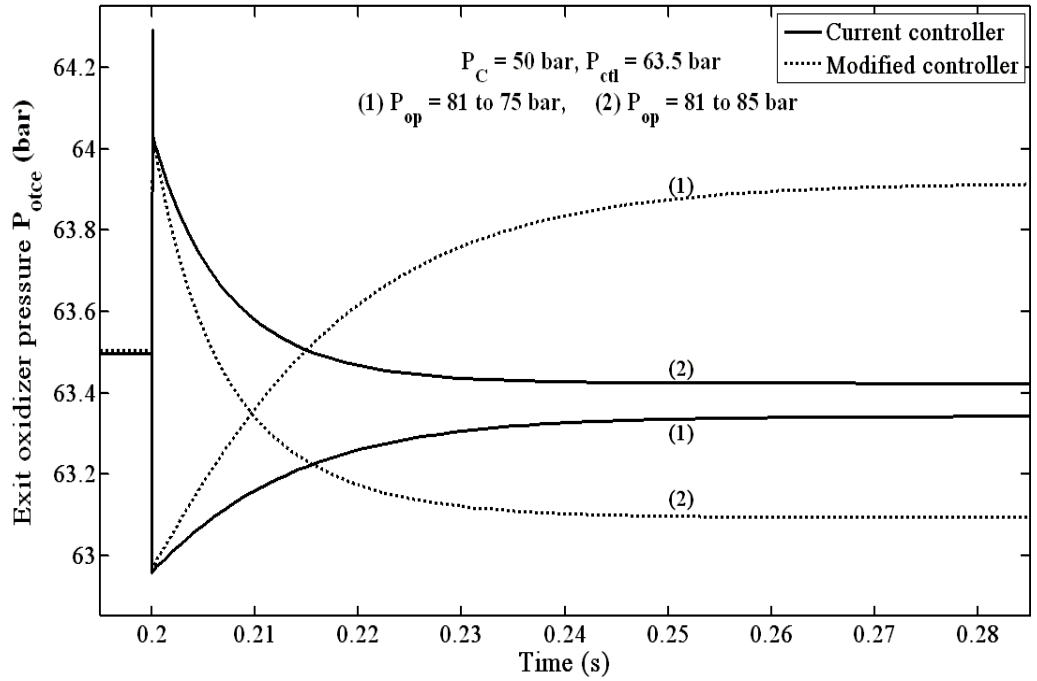

Fig. (8) Comparison between modified, and the current thrust controller responses due to input oxidizer pressure(P_{op}) step variation.

Figure (9) represents also a comparison between the two controllers due to combustion chamber pressure signal ($\mathbf{P_C}$) step variations. This figure also shows that the modified thrust controller would do the same action of the current thrust controller.

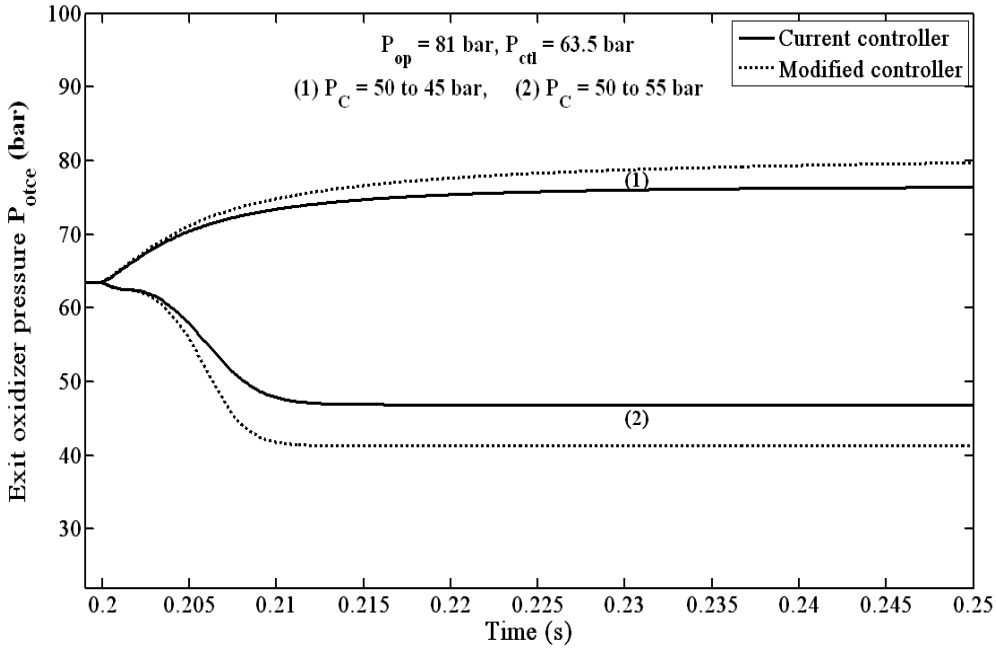

Fig. (9) Comparison between modified, and the current thrust controller responses due to combustion chamber pressure (P_C) step variation.

In conclusion the modified thrust controller works to do the same action of the current thrust controller in addition to continuous thrust modulation capability.

MODIFIED THRUST CONTROLLER INTEGRATED WITH EHSPC

By changing value of the controlling pressure inside the pressure chamber ($\mathbf{P_{ctl}}$), it is possible to control the exit oxidizer pressure ($\mathbf{P_{otce}}$), and exit oxidizer flow rate ($\mathbf{Q_{otce}}$). An (EHSPC) is connected to the modified thrust controller and the change in the controlling pressure ($\mathbf{P_{ctl}}$) is secured by changing the input current ($\mathbf{I_S}$), Fig (10). Continues modulation of the system could be performed through changing the input base current ($\mathbf{I_{BS}}$).

By communicating a positive value control current to the (EHSPC), the torque motor produces a torque proportional to the input control current. The resulting torque rotates the armature and flapper by relatively small angels. The hydraulic amplifier amplifies the very low energy mechanical signal into a large hydraulic energy output. The input supply pressure ($\mathbf{P_S}$) is decreased via the fixed orifice ($\mathbf{N_1}$), and the jet nozzles ($\mathbf{N_2}$). The displacement of the flapper plate changes the throttle area of the two regulating jet nozzles. The flapper motion to the right increases the area of the left nozzle and decreases the area of the right nozzle. The pressure ($\mathbf{P_{1S}}$) decreases and ($\mathbf{P_{2S}}$) increases, witch leads the spool to move and open the inlet port area ($\mathbf{B_S}$) [5-8]. Consequently, the controlling pressure value inside the pressure chamber ($\mathbf{P_{ctl}}$) is increased, reducing the hydraulic resistance of the valve. Arise in both outlet oxidizer pressure ($\mathbf{P_{otce}}$), and outlet oxidizer flow rate ($\mathbf{Q_{otce}}$) could occur and finally, after a

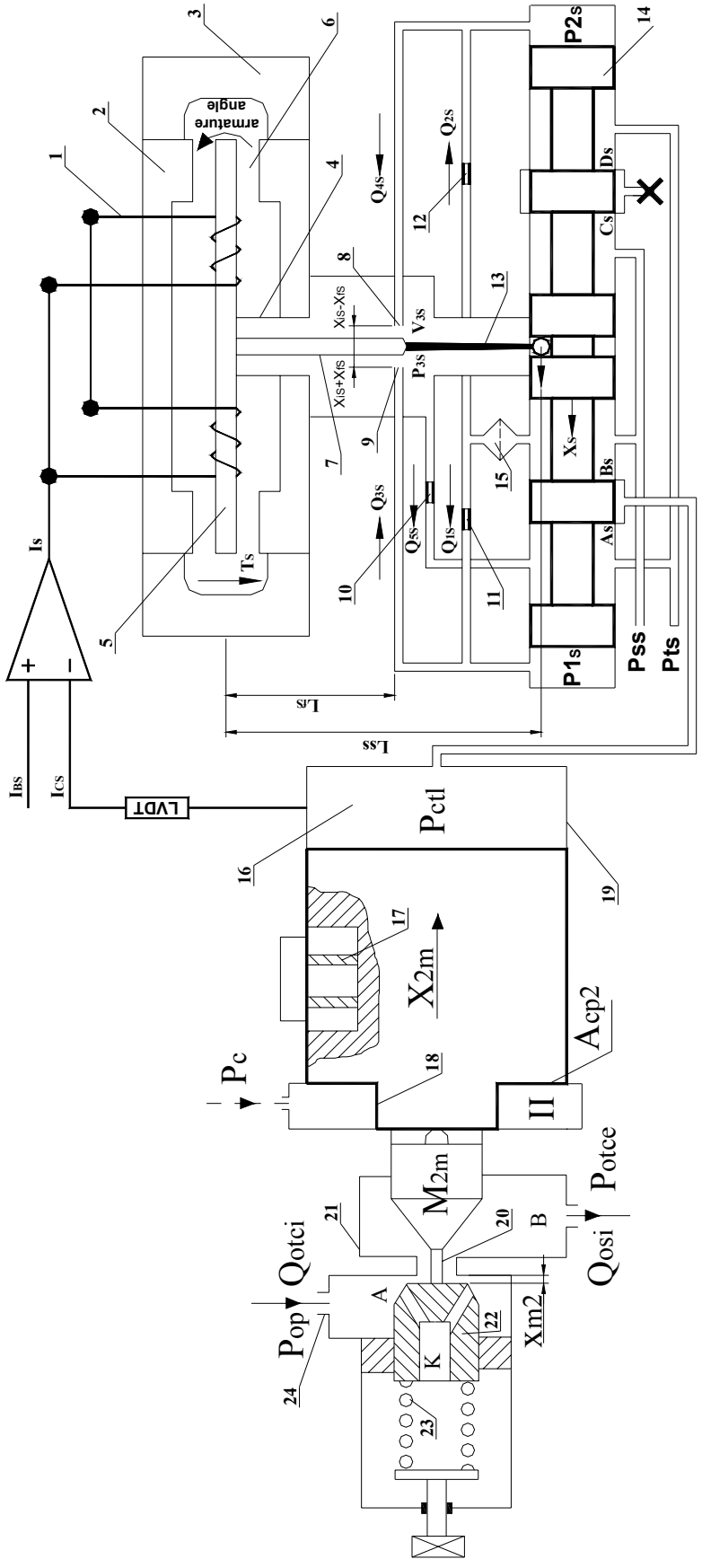

1- Control coiles; 2- Polar pieces; 3- Permenant magnet; 4- Flexible tube; 5- Armature; 6- Air gab; 7- Flapper plate; 8, 9- Two jet nozzles(N_2); 10,11, 12 - Fixed orifice(N_1); 13- Feedback wire; 14- Spool; 15- Fine filter; 16- Pressure chamber; 17- Limiter Half-rings; 18- Piston; 19- Casing; 19- Poppet; 21- Valve; 22- Auxiliary spring; 23- Connector for oxidizer inlet from pump;

Fig. (10) Integrated of EHSPC with Modified thrust controller scheme

sequence of operations the thrust increases. The opposite is true as a negative control current is applied

Then by a sequence of operations thrust of the (LPRE) under study increase. When the inlet current ($\mathbf{I_{BS}}$) to the (EHSPC) reversed the operation was reversed.

Mathematical model of the EHSPC integrated to the modified thrust controller may be described mathematically by the following non-linear equations.

$$T_s = K_{\theta s}\theta_s + K_{is}i_s \quad \textbf{(8)}$$

$$T_S = J_S\frac{d^2\theta_S}{dt^2} + f_{\theta S}\frac{d\theta_S}{dt} + K_{TS}\theta_s + T_{L1S} + T_{PS} + T_{FS} \quad \textbf{(9)}$$

$$T_{PS} = \frac{\pi}{4}d_{fS}^2(P_{2S} - P_{1S})L_{fS} \quad \textbf{(10)}$$

$$F_{SS} = K_{SS}(L_{SS}\theta + X_{SS}) \quad \textbf{(11)}$$

$$T_{FS} = F_{SS}L_{SS} = K_{SS}(L_{SS}\theta + X_{SS})L_{SS} \quad \textbf{(12)}$$

$$T_{L1S} = \begin{cases} 0 & |X_{fS}| < X_{fLS} \\ R_{fS}\dfrac{d\theta_S}{dt} - (|X_{fS}| - X_{fLS})K_{LfS}L_{fS}\,\text{sign}(\theta_S) & |X_{fS}| > X_{fLS} \end{cases} \quad \textbf{(13)}$$

$$Q_{1S} = C_dA_{oS}\sqrt{\frac{2}{\rho_{oS}}(P_{SS} - P_{1S})} = C_{12S}\sqrt{(P_{SS} - P_{1S})} \quad \textbf{(14)}$$

$$Q_{2S} = C_dA_{oS}\sqrt{\frac{2}{\rho_{oS}}(P_{SS} - P_{2S})} = C_{12S}\sqrt{(P_{SS} - P_{2S})} \quad \textbf{(15)}$$

$$Q_{3S} = C_d\pi d_{fS}(X_{iS} + X_{fS})\sqrt{\frac{2}{\rho_{oS}}(P_{1S} - P_{3S})} = C_{34S}(X_{iS} + X_{fS})\sqrt{(P_{1S} - P_{3S})} \quad \textbf{(16)}$$

$$Q_{4S} = C_d\pi d_{fS}(X_{iS} - X_{fS})\sqrt{\frac{2}{\rho_{oS}}(P_{2S} - P_{3S})} = C_{34S}(X_{iS} - X_{fS})\sqrt{(P_{2S} - P_{3S})} \quad \textbf{(17)}$$

$$X_{fS} = L_{fS}\theta_S \quad \textbf{(18)}$$

$$Q_{5S} = C_dA_{5S}\sqrt{\frac{2}{\rho_{oS}}(P_{3S} - P_{TS})} = C_{5S}\sqrt{P_{3S} - P_{TS}} \quad \textbf{(19)}$$

$$Q_{1S} - Q_{3S} + A_{SS}\frac{dX_S}{dt} = \frac{d}{dt}\left[\frac{V_o - A_{SS}X_S}{B_{oil}}P_{1S}\right] \quad \textbf{(20)}$$

$$Q_{2S} - Q_{4S} - A_{SS}\frac{dX_S}{dt} = \frac{d}{dt}\left[\frac{V_o + A_{SS}X_S}{B_{oil}}P_{2S}\right] \quad \textbf{(21)}$$

$$Q_3 + Q_4 - Q_5 = \frac{d}{dt}\left[\frac{V_{3S}}{B_{oil}}P_{3S}\right] \quad \textbf{(22)}$$

$$A_{SS}(P_{2S} - P_{1S}) = m_{SS}\frac{d^2X_S}{dt^2} + f_{SS}\frac{dX_S}{dt} + F_{jS} + F_{SS} \quad \textbf{(23)}$$

$$F_{jS} = \begin{cases} \dfrac{\rho_{oil}{Q_{BS}}^2}{C_CA_{BS}} + \dfrac{\rho_{oil}{Q_{DS}}^2}{C_CA_{DS}} & \text{for } X_S > 0 \\ \dfrac{\rho_{oil}{Q_{AS}}^2}{C_CA_{AS}} + \dfrac{\rho_{oil}{Q_{CS}}^2}{C_CA_{CS}} & \text{for } X_S > 0 \end{cases} \quad \textbf{(24)}$$

$$\left.\begin{aligned} A_{AS} &= A_{CS} = \omega\Delta_S \\ A_{BS} &= A_{DS} = \omega\sqrt{{X_S}^2 + {\Delta_S}^2} \end{aligned}\right\} \quad \text{for } X \geq 0 \quad \textbf{(25)}$$

$$\left.\begin{aligned} A_{AS} &= A_{CS} = \omega\sqrt{X_S{}^2 + \Delta_S{}^2} \\ A_{BS} &= A_{DS} = \omega\Delta_S \end{aligned}\right\} \quad \text{for} \quad X \le 0 \tag{26}$$

$$Q_{AS} = C_d A_{AS}(X_S)\sqrt{\frac{2}{\rho_{oil}}(P_{ctl} - P_{tS})} \tag{27}$$

$$Q_{BS} = C_d A_{BS}(X_S)\sqrt{\frac{2}{\rho_{oil}}(P_{SS} - P_{ctl})} \tag{28}$$

$$Q_{BS} - Q_{AS} + A_P\frac{dX_{2m}}{dt} = \frac{d}{dt}\left[\frac{V_{CS} - A_P X_{2m}}{B_{oil}}P_{ctl}\right] \tag{29}$$

$$Q_{otci} = C_d \pi d_v (X_{m2} - X_2)\sqrt{\frac{2}{\rho_o}(P_{op} - P_{otce})} \tag{30}$$

$$Q_{osi} = K_d\sqrt{P_{otce} - P_{og}} \tag{31}$$

$$Q_{otci} - Q_{osi} - A_N\frac{dX_2}{dt} - \frac{V_{e2}}{B}\frac{dP_{otce}}{dt} = 0 \tag{32}$$

$$P_C A_{cp2} + P_{otce}A_{e2} + P_{op}A_{i2} = M_{2m}\frac{d^2X_{2m}}{dt^2} + f_2\frac{dX_{2m}}{dt} + P_{ctl}A_P - F_{L2m} \tag{33}$$

$$F_{LL2m} = \begin{cases} |X_{2m}|K_{L2} - f_{L2}\dfrac{dX_{2m}}{dt} & X_{2m} \le 0 \\ 0 & X_{2m} > 0 \end{cases} \tag{34}$$

$$F_{LR2m} = \begin{cases} (X_{2m} - X_{m2})K_{L2} + f_{L2}\dfrac{dX_{2m}}{dt} & X_{2m} \ge X_{m2} \\ 0 & X_{2m} < X_{m2} \end{cases} \tag{35}$$

$$F_{L2m} = F_{LL2m} - F_{LR2m} \tag{36}$$

Simulation

Figures (11) to (14) show a simulation sample of, the (EHSPC) integrated to the modified thrust controller. These figures show respectively the controllers exit oxidizer pressure (**P_{otce}**) variation with step variations of combustion chamber pressure signal (**P_C**), inlet oxidizer pump pressure (P_{op}), input controlling current (**I_{BS}**), and the change of the integrated system controller form the first rating to the second rating.

It can be seen from Figs. 11-13 that the integrated system of the modified thrust controller with EHSPC has almost the same behavior as the current thrust controller. Moreover, a continues modulation could be reached by changing the input control current (**I_{BS}**).

Responses associated with switching from a thrust rating to another rating are shown in Fig (14) for the current controller and the modified system. Nearly identical responses have been demonstrated.

Table (2) represents a comparison between the current controller and the integrated system from points of view of response type, settling time, and steady state error. The two controllers showed over-damped responses and nearly zero steady state error. A higher settling time was noticed with the integrated system, but this can be attributed to the complexity of the added system, nonlinear model behavior, and the limited

computational capabilities. However, from practical point of view, this can be considered acceptable as a simulation result.

Table (2) Comparison between current and modified integrated system controller

Parameter	Current controller	Integrated system
Response type	Over-damped	Over-damped
Settling time	40 ms	500 ms
Steady state error	Nearly zero	Nearly zero

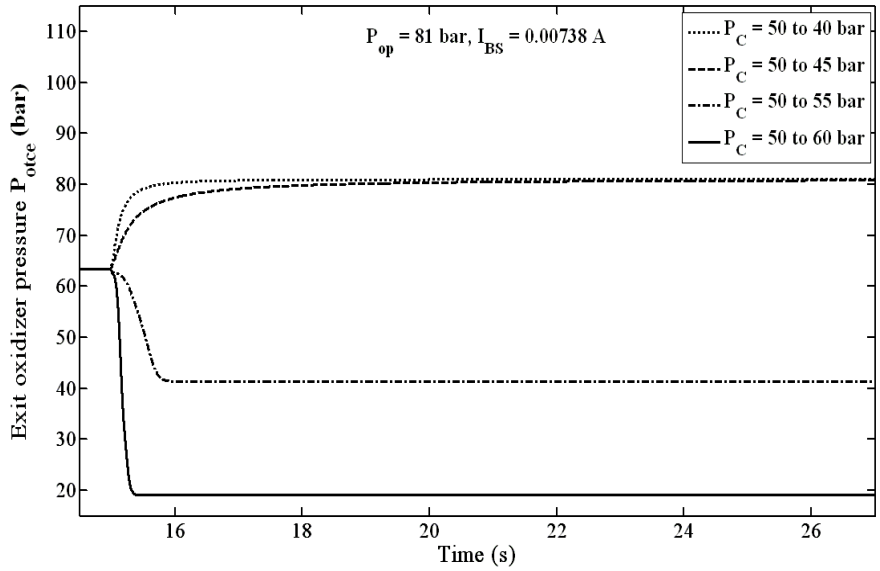

Fig. (11) Response of the EHSPC integrated to the modified thrust controller due to combustion chamber pressure signal (P_C) step variation.

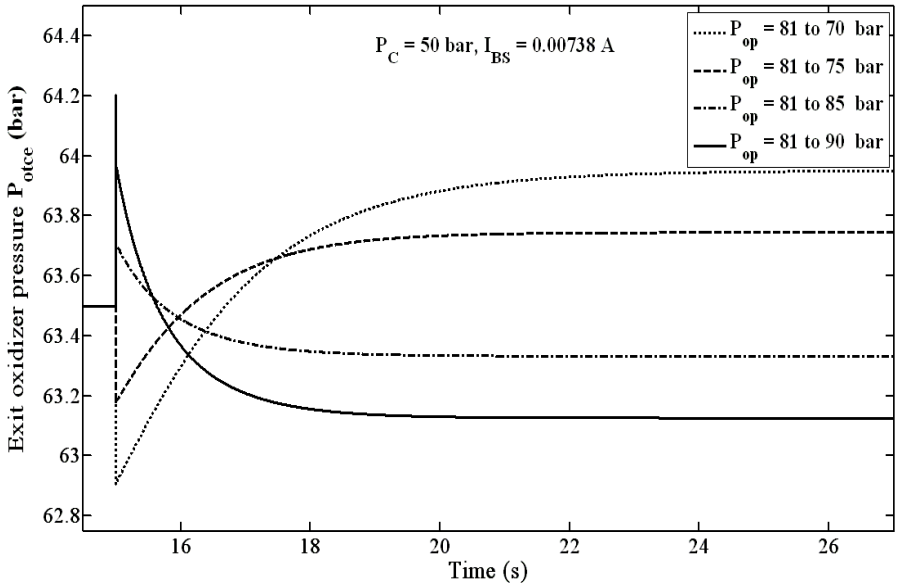

Fig. (12) Response of the EHSPC integrated to the modified thrust controller due to input oxidizer pump pressure (P_C) step variation.

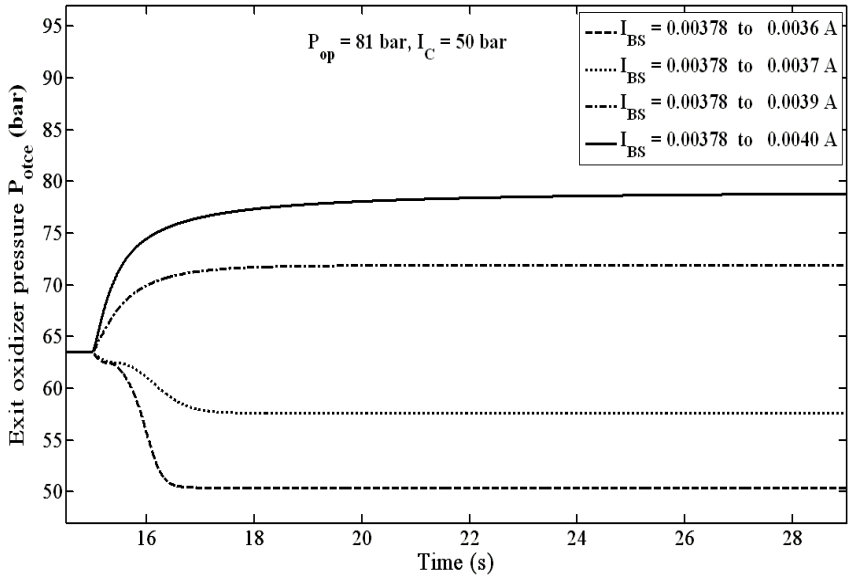

Fig. (13) Response of the EHSPC integrated to the modified thrust controller due to input controlling current (I_{BS}) step variation.

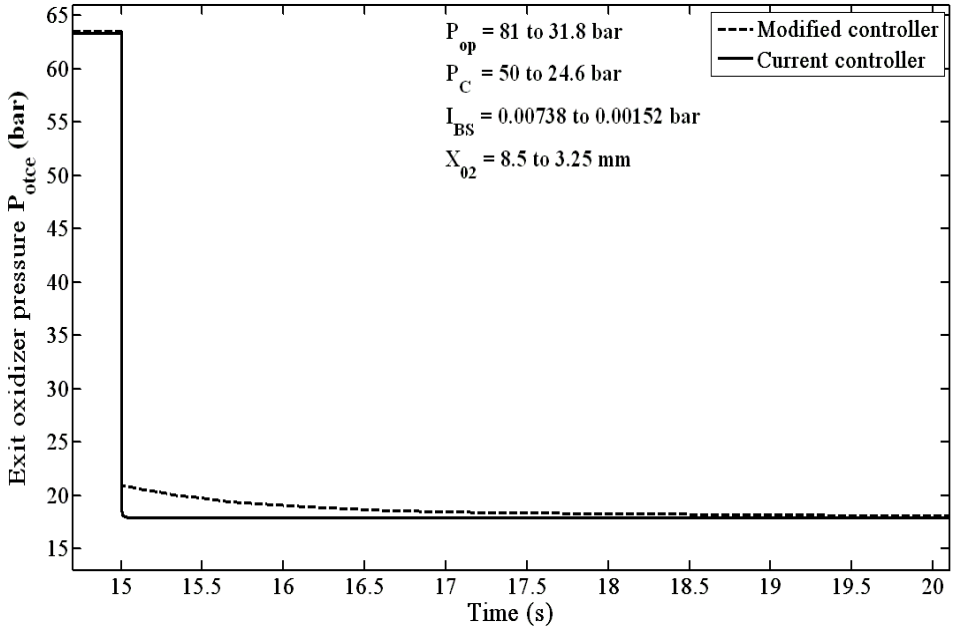

Fig. (14) Response of the EHSPC integrated to the modified thrust controller due to change in thrust rating.

CONCLUSIONS

The thrust controller of a liquid propellant rocket engine was analyzed and simulated using the SIMULINK simulation program. It was proven that the system is stable during the two power ratings and the transition from the first to the second rating. A modification of the thrust controller has been carried out to secure a continuous thrust modulation. The thrust controller design, after modification, was capable to operate at the same operating conditions and to perform the same function of the current thrust controller. The modified thrust controller is then integrated with (EHSPC) and it showed

the same behavior as that before modification. It has the advantage that a continuous thrust modulation could be obtained by changing the input controlling current. The comparison between existing controller, modified controller, and the modified system incorporating the modified controller integrated with (EHSPC) was based on the response to input step pressure variation in each case. As compared with the current thrust controller, the modified system showed a slightly higher time delay. However, considering system complexity, nonlinear model behavior, and computational limitations, this delay can be considered practically acceptable as a simulation result. The implemented system can be considered as a powerful means to fulfill reliably the requirements imposed at many situations where the thrust modulation is needed.

REFERENCES

1. Timnat, Y. M., “Advanced Chemical Rocket Propulsion”, 1987.
2. David, H. Huang; “Modern Engineering for Design of Liquid Propellant Rocket Engine”, 1992.
3. Tamer, N. M., “Dynamic Behavior of Control Valves Of a Liquid Propellant Rocket Engine Feeding Assembly” M.Sc. Thesis, Military Technical College, Cairo, 2006.
4. Tamer, N. M., “Investigation of Dynamic Behavior of Feeding System of Liquid Propellant Rocket Engine” M.Sc. Thesis, Military Technical College, Cairo, 2003.
5. Rabie, M. G., “Fluid Power Engineering”, Cairo, 2006.
6. Yeaple, F., “Fluid Power Design hand book”, Second Edition, 1990.
7. Metwally, M., Rabie, M. G., Abdou, S. E., “Dynamic Perforamnce of an Electro-hydraulic Servo-Actuator with Contactlees Controlled Spool”, Military Technical College, Cairo, 2006.
8. El-Sayed, A. A., Gobran, M. H., Rabie, M. G., “Investigation of Characteristics of an Electro-hydraulic Servo-Actuator Incorporating Jet Pipe Amplifier”, Military Technical College, Cairo, 2003.
9. Rabie, M. G., Ibrahim, U. M., “Modeling and Simulation of a Compact Electro-hydraulic Servo-Actuator”, Cairo Univ., 1990.